Supplementary material for the manuscript entitled:

"Near-zero-index media as electromagnetic ideal fluids"

Iñigo Liberal[1,2*], Michaël Lobet[3,*], Yue Li[4], Nader Engheta[5]

[1]*Electrical and Electronic Engineering Department, Universidad Pública de Navarra, Campus Arrosadía, Pamplona, 31006 Spain*

[2]*Institute of Smart Cities, Universidad Pública de Navarra, Campus Arrosadía, Pamplona, 31006 Spain*

[3]*Spatial de Liège, Avenue du Pré-Aily, B-4031 Angleur, Belgium*

[4]*Department of Electronic Engineering, Tsinghua University, Beijing 100084, China*

[5]*Department of Electrical and Systems Engineering, University of Pennsylvania, Philadelphia, PA 19104, USA*

** These authors contributed equally to this work.*

Supplementary Note 1: Impact of loss in the electromagnetic power flow distribution

In this supplementary note we provide additional information on the impact of loss in the electromagnetic power flow distribution, and the behavior of NZI media as an electromagnetic ideal fluid. The role of material loss in the power flow distribution can be analyzed by inspecting the expressions for the divergence $\nabla \cdot \mathbf{S}_{\mathrm{R}} = -\frac{\omega}{2}(\varepsilon_0 \varepsilon'' |\mathbf{E}|^2 + \mu_0 \mu'' |\mathbf{H}|^2)$ and curl $\nabla \times \mathbf{S}_{\mathrm{R}} = -\frac{1}{2}\mathrm{Re}[(\mathbf{E} \cdot \nabla)\mathbf{H}^*]$ of the power flow (for TM waves exciting a two-dimensional system). It is clear from these equations that the presence of loss directly induces a nonzero divergence on the power flow, proportional to the imaginary part of the permittivity and/or permeability, and that can be associated with the field decay. On the other hand, the impact of loss on the curl of the power flow indirectly comes from the fact that the magnetic field is no longer uniform, and consequently makes it difficult to predict analytically.

Intuitively, one can understand that the lack of vorticity is more robust in the presence of loss than the divergenceless property of the power flow. First, since deviations from a nonzero curl are induced by spatial variations of the magnetic field, the curl can be expected to be small as long as the fields are stretched as compared to the free-space wavelength in the NZI limit. Secondly, the term $(\mathbf{E} \cdot \nabla)\mathbf{H}^*$ implies that only the field variations along the electric field contribute to the curl of the power flow. Therefore, for fields similar to a plane wave, the spatial variation induced by the decay along the direction of propagation does not contribute to the vorticity of the power flow.

However, field distributions observed in arbitrary geometries are complex, thus in general implying a complex interplay between material loss and vorticity. This effect can be addressed numerically, and Figs. S1-S2 provide an in-depth analysis on how different degrees of material loss affect the predictions for the configuration corresponding to Fig. 2 of the main text.

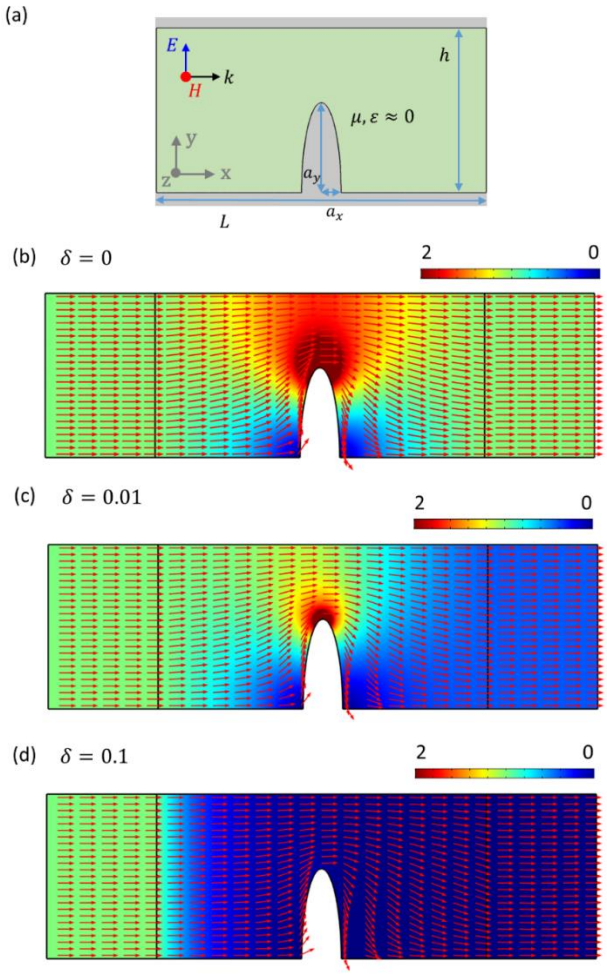

Fig. S1. Impact of loss in the electromagnetic power flow distribution (vectorial plot). (a) Sketch of the geometry: a 2D lossy EMNZ waveguide, $\varepsilon = \mu = i\,\delta$, of height $h = 3\lambda_p$ containing a deformed section modeled as a half-ellipse with semiaxes $a_y = a_1 + a_2^2/a_1$ and $a_x = a_1 - a_2^2/a_1$ with $a_1 = 2.5\,\lambda_p$ and $a_2 = 0.8\,\lambda_p$. All waveguide walls are considered as PEC boundaries, and λ_p is the free-space wavelength at the NZI frequency. **(b)-(d)** amplitude and vector plot of the real part of the time-averaged Poynting vector field ($\mathbf{S}_R$, power flow), normalized to their incident counterparts, for a loss parameter of **(b)** $\delta = 0$ (lossless), **(c)** $\delta = 0.01$, and **(d)** $\delta = 0.1$. These numerical results illustrate that the magnitude of the power flow exhibits an exponential decay in lossy EMNZ media. However, the normalized vectorial distribution is robust against the presence of dissipation damping, and the absence of vorticity is preserved in the parameter range studied here. The considered loss factors are realistic of metamaterial implementations of NZI media including dispersive waveguides and all-dielectric photonic crystals, and some of the highest-quality ENZ continuous media, like silicon carbide (SiC), characterized by $\varepsilon_{ENZ} = i0.03$. However, other implementations like those based on doped semiconductor exhibit higher losses $\varepsilon_{ENZ} = i0.2\sim0.5$.

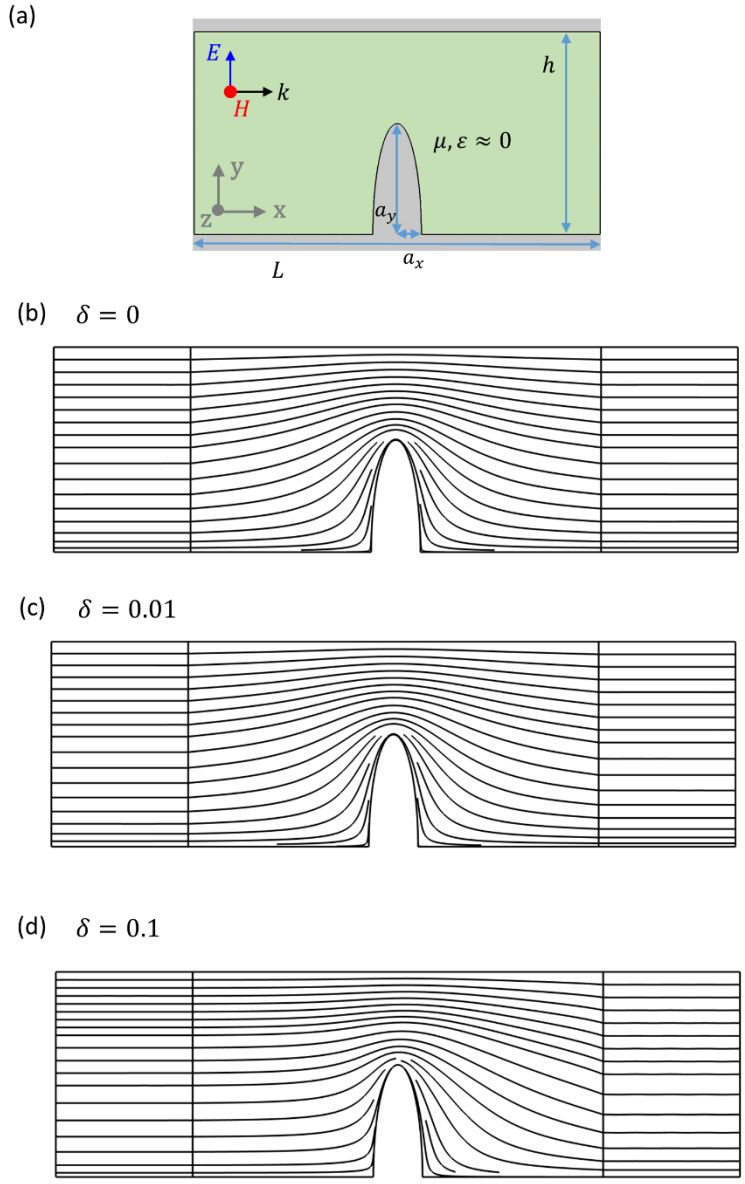

Fig. S2. Impact of loss in the electromagnetic power flow distribution (streamlines). (a) Sketch of the geometry: a 2D lossy EMNZ waveguide, $\varepsilon = \mu = i\,\delta$, of height $h = 3\lambda_p$ containing a deformed section modeled as a half-ellipse with semiaxes $a_y = a_1 + a_2^2/a_1$ and $a_x = a_1 - a_2^2/a_1$ with $a_1 = 2.5\,\lambda_p$ and $a_2 = 0.8\,\lambda_p$. All waveguide walls are considered as PEC boundaries, and λ_p is the free-space wavelength at the NZI frequency. **(b)-(d)** streamlines of the real part of the time-averaged Poynting vector field ($\mathbf{S}_R$, power flow), normalized to their incident counterparts, for a loss parameter of **(b)** $\delta = 0$ (lossless), **(c)** $\delta = 0.01$, and **(d)** $\delta = 0.1$. These numerical results illustrate that streamlines of the power flow are very robust against dissipation damping, and the absence of vorticity is preserved.

Supplementary Note 2: Frequency response of the electromagnetic power flow distribution

This supplementary note provides a numerical analysis of the frequency response of the power flow distribution in the NZI limit. To this end, we define material parameters with a Lorentzian dispersion profile model $\mu(\omega) = \varepsilon(\omega) = \left(\omega^2 - \omega_p^2\right)/(\omega^2 - \omega_0^2)$ with $\omega_0 = 0.9\ \omega_p$, and with a group velocity of $v_g(\omega_p) = (c/2)\left(1 - \omega_0^2/\omega_p^2\right) = 0.095c$. Fig. S2 shows the power flow distributions at frequencies $\omega = 0.97\ \omega_p$, $0.99\ \omega_p$, $1\ \omega_p$, $1.01\ \omega_p$ and $1.03\omega_p$. These numerical results demonstrate that the behavior of NZI media as an electromagnetic ideal fluid is a well-behaved frequency limit. In other words, it does not correspond to a singular frequency point, but the vorticity in the power flow is inhibited in a finite bandwidth where the material parameters can be considered sufficiently small, while vortices of the power flow appear as one get further from the NZI frequency.

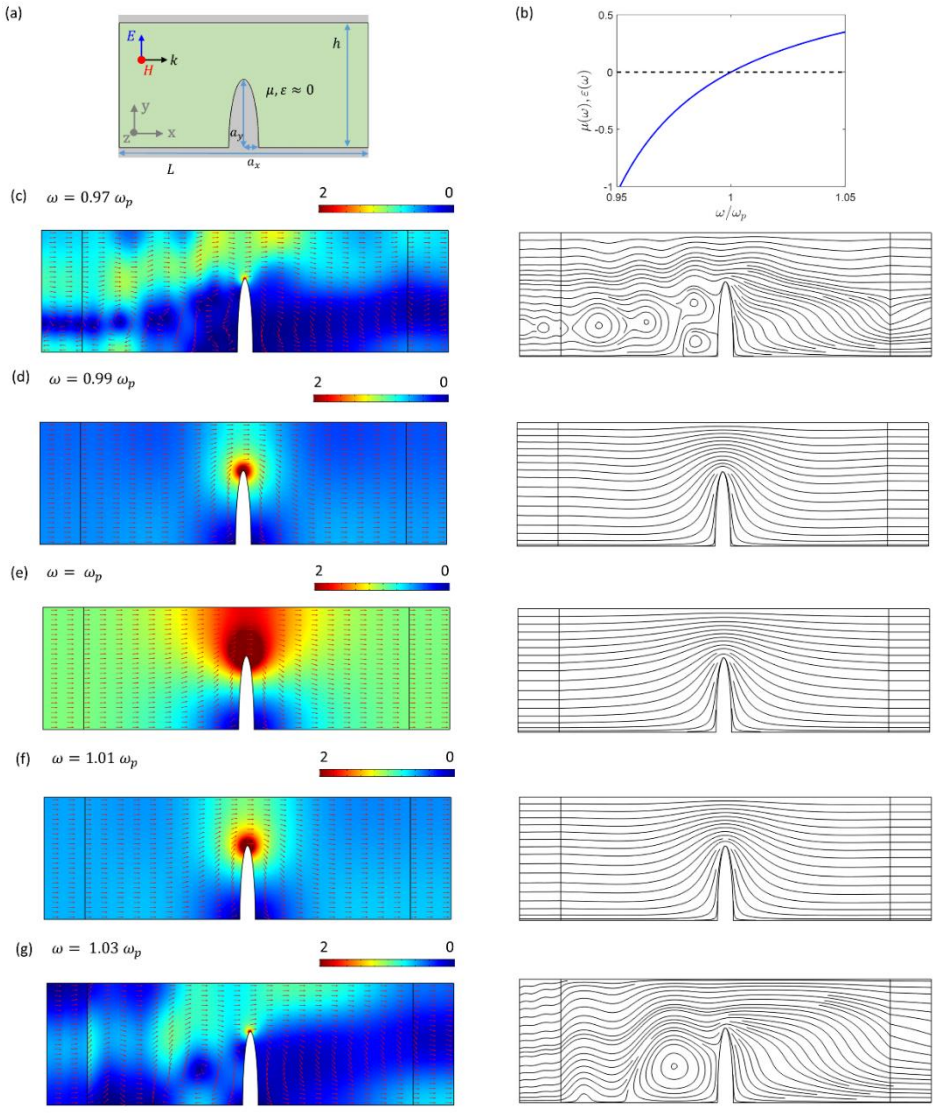

Fig. S3. Frequency response of the electromagnetic power flow distribution. (a) Sketch of the geometry: a 2D EMNZ waveguide of height $h = 3\lambda_p$ containing a deformed section modeled as a half-ellipse with semiaxes $a_y = a_1 + a_2^2/a_1$ and $a_x = a_1 - a_2^2/a_1$ with $a_1 = 2.5\ \lambda_p$ and $a_2 = 0.8\ \lambda_p$. All

waveguide walls are considered as PEC boundaries, and λ_p is the free-space wavelength at the NZI frequency. **(b)** Dispersion profile of the permittivity and permeability, following a Lorentz model $\mu(\omega) = \varepsilon(\omega) = \left(\omega^2 - \omega_p^2\right)/(\omega^2 - \omega_0^2)$ with $\omega_0 = 0.9\,\omega_p$ and with a group velocity of $v_g(\omega_p) = (c/2)\left(1 - \omega_0^2/\omega_p^2\right) = 0.095c$. **(c)-(f)** (Left) Amplitude and vector plot of the real part of the time-averaged Poynting vector field ($\mathbf{S}_R$, power flow), normalized to their incident counterparts, and (right) streamlines, at different frequencies **(c)** $\omega = 0.97\,\omega_p$, **(d)** $\omega = 0.99\,\omega_p$, **(e)** $\omega = \omega_p$, **(f)** $\omega = 1.01\,\omega_p$ and **(g)** $\omega = 1.03\,\omega_p$. These numerical results illustrate that the vorticity in the power flow is inhibited in a finite bandwidth where the material parameters can be considered sufficiently small.

Supplementary Note 3: The role of the permeability

As it is demonstrated in the main text, the power flow in an ENZ medium has the same spatial distribution independently of the value of its permeability μ except for a global scalar factor. For the typical supercoupling configuration, consisting of two identical TEM waveguides of height h, connected by an arbitrarily shaped ENZ region of area A, the scalar factor reduces to $|H_z^{cst}|^2 = \left|1 + i\frac{\omega}{c}\frac{A}{2h}\mu\right|^{-2}$. To illustrate this fact, Fig. S4 represents the power flow for the configuration studied in Fig. 1, but for different values of the relative permeability. Fig. S5 represents the same results, but when the color scale has been normalized to the global scalar factor $|H_z^{cst}|^2$. Finally, Fig. S6 shows the streamlines of the power flow for different values of the relative permeability.

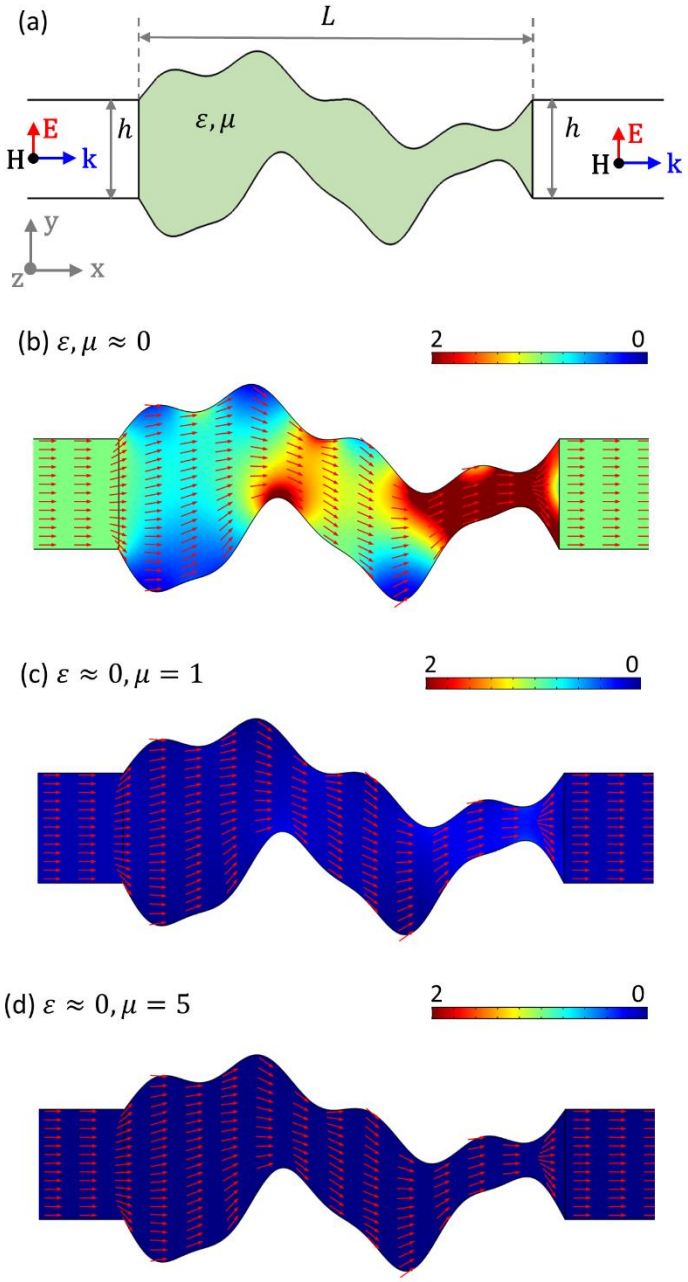

Fig. S4. Electromagnetic power flow distribution as a function of the relative permeability of the epsilon-near-zero (ENZ) (vectorial plot). (a) Sketch of the geometry: a two-dimensional (2D) waveguide of height $h = 0.25\lambda$ containing a deformed section of length $L = \lambda$, filled with a material with relative permittivity ε and permeability μ. λ is the free-space wavelength at the frequency of the incoming wave. **(b)-(d)** Amplitude and normalized vector plot of the real part of the time-averaged Poynting vector field ($\mathbf{S}_R$, power flow) when the waveguide is filled with an ENZ medium, $\varepsilon \approx 0$, with a relative permeability of **(b)** $\mu \approx 0$, i.e., epsilon-and-mu-near-zero (EMNZ) media, **(c)** $\mu \approx 1$ and **(d)** $\mu \approx 5$. The numerical results illustrate that the magnitude of the power flow decreases as the permeability increases, but the normalized vectorial distribution is independent of the value of the relative permeability.

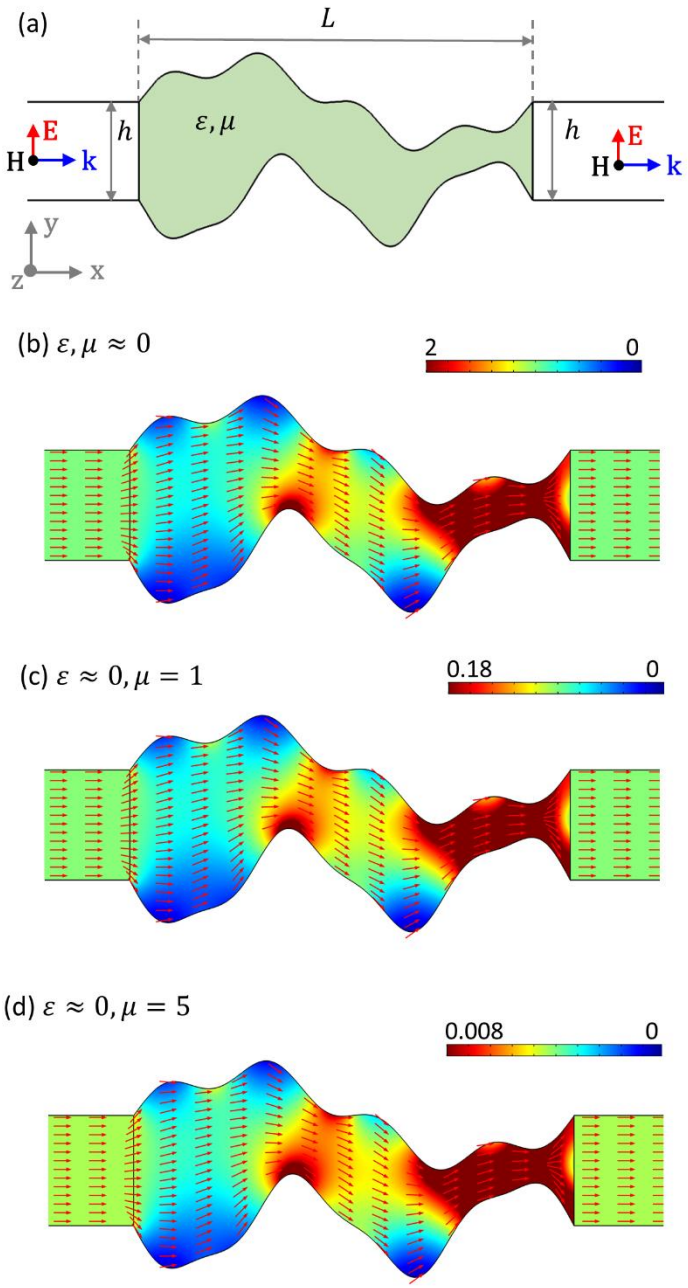

Fig. S5. Electromagnetic power flow distribution as a function of the relative permeability of the epsilon-near-zero (ENZ) (vectorial plot with adjusted colorbars). (a) Sketch of the geometry: a two-dimensional (2D) waveguide of height $h = 0.25\lambda$ containing a deformed section of length $L = \lambda$, filled with a material with relative permittivity ε and permeability μ. λ is the free-space wavelength at the frequency of the incoming wave. **(b)-(d)** Amplitude and normalized vector plot of the real part of the time-averaged Poynting vector field ($\mathbf{S}_R$, power flow) when the waveguide is filled with an ENZ medium, $\varepsilon \approx 0$, with a relative permeability of **(b)** $\mu \approx 0$, i.e., epsilon-and-mu-near-zero (EMNZ) media, **(c)** $\mu \approx 1$ and **(d)** $\mu \approx 5$. The colobars on each figure have been adjusted to the value, $2|H_z^{\text{cst}}|^2$, with $H_z^{\text{cst}} = \left(1 - i\frac{1}{2}\frac{\omega}{c}\mu L\right)^{-1}$. The numerical results illustrate that the power flow distribution is independent of the value of the relative permeability, except for a scalar factor $|H_z^{\text{cst}}|^2$.

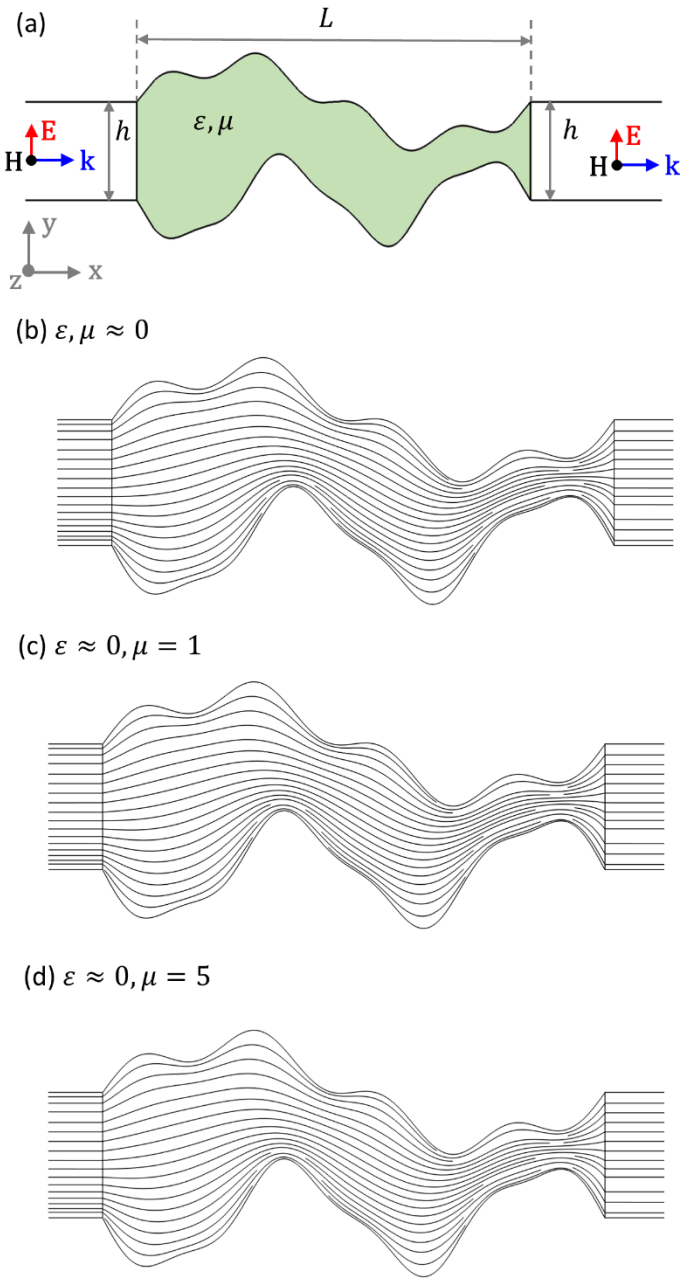

Fig. S6. Electromagnetic power flow distribution as a function of the relative permeability of the epsilon-near-zero (ENZ) (streamlines). (a) Sketch of the geometry: a two-dimensional (2D) waveguide of height $h = 0.25\lambda$ containing a deformed section of length $L = \lambda$, filled with a material with relative permittivity ε and permeability μ. λ is the free-space wavelength at the frequency of the incoming wave. **(b)-(d)** Streamlines of the real part of the time-averaged Poynting vector field ($\mathbf{S}_R$, power flow) when the waveguide is filled with an ENZ medium, $\varepsilon \approx 0$, with a relative permeability of **(b)** $\mu \approx 0$, i.e., epsilon-and-mu-near-zero (EMNZ) media, **(c)** $\mu \approx 1$ and **(d)** $\mu \approx 5$. The numerical results illustrate that the streamlines of the power flow are independent of the value of the relative permeability.